STRUCTURE OF GLASS

Symposium

Harokopio University, Athens, Greece
29-31 May, 2001

Edited by

George Kordas
NCSR Demokritos
Athens, Greece

Panayota Chrysicopoulou
Harokopio University
Athens, Greece

ΕΚΔΟΤΙΚΟΣ ΟΜΙΛΟΣ ΙΩΝ
ΕΚΔΟΣΕΙΣ ΙΩΝ
Συμπληγάδων 7, 12131, Περιστέρι
τηλ.: 010.57.47.729, 010.57.68.853, FAX: 010. 57.51.438
e-mail address: ion_publ@hol.gr, http://www.iwn.gr
Βιβλιοπωλείο: Σόλωνος 85, 10679, Αθήνα
τηλ.: 010.33.87.570, FAX: 010.33.87.571

LOCAL STRUCTURE AND SPECTROSCOPY OF METAL IONS IN GLASS

Efstratios I. Kamitsos

Theoretical and Physical Chemistry Institute,
National Hellenic Research Foundation,
48 Vass. Constantinou Ave., Athens 116 35, Greece

ABSTRACT

This paper reviews far-infrared spectroscopy results regarding the nature of metal ion sites in alkali and alkaline earth borate glasses. It was proposed that the far-infrared data can be understood in a unified way which is based on the presence of at least two types of site, i.e., singly- and doubly-occupied sites for metal ions. The study of Li borate glasses by molecular dynamics simulations helps to elucidate the nature of the local borate units constituting the two types of site, and to correlate the type of sites with the Li ion-site vibrational response in the far-infrared. The distinction between different types of site in glasses can be made on the basis on the number of non-bridging oxygen atoms involved in the coordination sphere of metal ion. Experimental results from UV probe ion spectroscopy on sodium borate glasses were discussed in terms of the 'two-site' model.

1. INTRODUCTION

The short-range order structures of the glass network and the local environments which host the modifier metal ions are very often discussed independently. However, during glass formation a synergy develops between the requirements of metal ions for the establishment of suitable coordination environments/sites and the ability of the glass network to provide such anionic sites. In the case of crystallisation, additional constraints are imposed by the need to establish also long-range structural periodicity. As the glass state is approached, thermodynamics drives the system towards the stable crystalline state but kinetics prohibits it from reaching the crystalline structure. Therefore, although the natural tendency for metal ions is to create in glass 'crystal-like' sites, i.e., sites similar to those in the corresponding crystal, there is a strong possibility that additional sites are created for metal ions because of the disordered nature of the glassy state. The nature of metal ion sites and their spatial distribution are important factors determining the physical properties of glass.

Current ideas about glass structure originate mainly from the continuous random network (CRN) model developed by Zachariasen [1] and extended to alkali silicate glasses by Warren and Biscoe [2]. The classical two-dimensional representation of the Warren-Biscoe and Zachariasen model for a sodium silicate glass is shown in Figure 1(a). In pure silica glass each silicon atom is coordinated to four oxygen atoms in a three dimensional network of SiO_4 tetrahedra, which are connected to each other randomly through Si-O-Si bridging bonds. The addition of alkali metal oxide to pure SiO_2 breaks Si-O-Si bonds and forms two negatively charged non-bridging oxygen (NBO) atoms for every oxygen atom of added modifier metal oxide, with each NBO being compensated by an alkali metal ion. Compared to the well defined Si-O coordination environment, the CRN model does not impose any constraints on the environment of the alkali metal ions in glass, which are considered to be homogeneously distributed in various voids/sites of the disordered silicon-oxygen network [2].

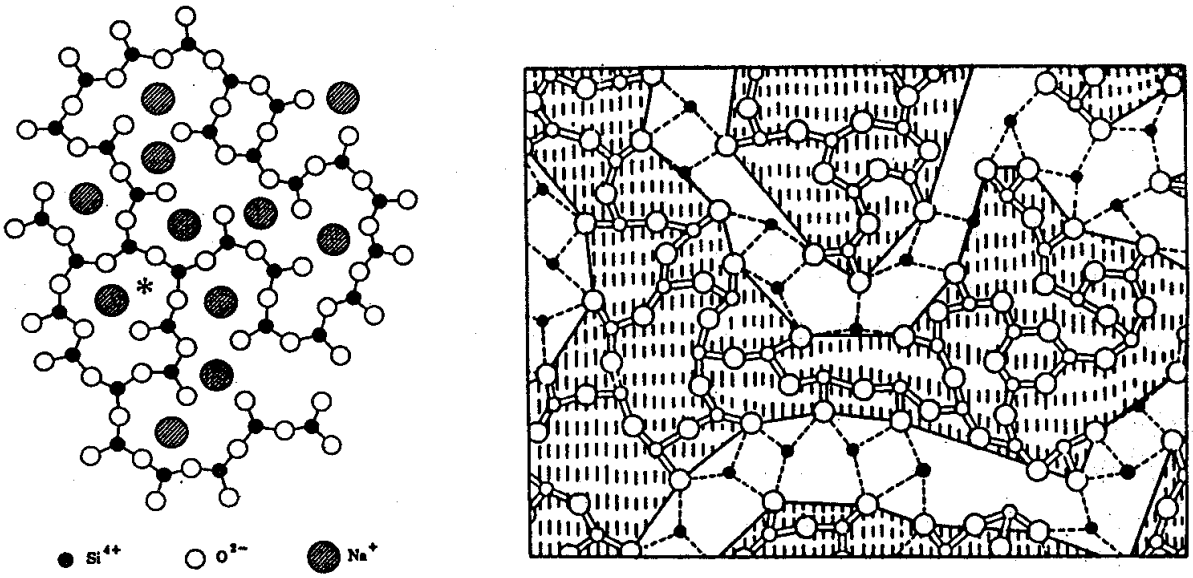

Figure 1. (a) Schematic two-dimensional representation of the structure of a sodium silicate glass according to the continuous random network (CRN) model of Zachariasen [1] as extended to modified silicates by Warren and Biscoe [2]. (b) A two-dimensional diagram of the modified random network (MRN) model proposed by Greaves [3] for the structure of an oxide glass M_2O_3-$2G_2O_3$ (M = modifying cation, G_2O_3 = glass forming oxide). The shaded regions represent the unmodified part of the glass network, where G-O covalent bonds are shown by double solid lines. The modifying metal cations (solid circles) are microsegregated from the G-O network and are coordinated predominantly to non-bridging oxygen atoms with ionic M-O bonds (dashed lines).

On the basis of extended X-ray absorption fine structure (EXAFS) studies on sodium silicate glasses Greaves [3] has developed the 'modified random network' (MRN) model. According to the MRN model for silicates, the continuous random network of bridged SiO_4 tetrahedra in pure silica is significantly altered by the modifying metal cations (e.g. Na^+) which are not spread uniformly throughout the glass. Instead, the metal ions are proposed to be microsegregated between the bridged SiO_4 units to which they are linked through the NBO atoms, Figure 1(b). Thus, the key difference between MRN and the earlier CRN model for silicates is the presence of the modifier metal ions within a sublattice composed mainly of NBO's. Greaves [3] argued that the formation of regions rich in alkali/NBO leads to a more favourable alkali-NBO coordination resembling the alkali-oxygen ordering in crystalline structures.

Considerable ordering in the coordination environment of modifier cations in glass has been shown also by Gaskell et al. [4] on the basis of neutron diffraction studies in a Ca-silicate glass. It was demonstrated that Ca^{2+} ions are coordinated by six oxygen atoms, and that the Ca-O octahedra are interconnected

by sharing edges in arrangements characteristic of the corresponding c-$CaSiO_3$ crystal. In addition, molecular dynamics (MD) simulations [5] of alkali silicate glasses showed nanoscale inhomogeneity of glass structure in accordance with the MRN model. At low alkali metal concentrations alkali ions and NBO's were shown to be aggregated rather than being uniformly dispersed in the glass structure. As the alkali content increases, the alkali/NBO rich regions grow in size and percolate through the bulk of the glass to form microchannels or pathways suitable for ion conduction. In a recent study of alkali silicate glasses by thermodynamics, MD simulations and neutron diffraction experiments, Vedishcheva et al. [6] investigated the distribution of the silicate Si^n species (with n bridging oxygen, BO, atoms per Si) and of the network modifying cation environments. They concluded that, contrary to what may be expected from the MRN model, the Si^4 species do not tend to aggregate but rather to be more uniformly distributed in the glass network. Similarly, recent solid state NMR studies on alkali silicate glasses [7] suggest a near-uniform spatial distribution of alkali ions.

As presented above, the nature of metal ion sites and their spatial distribution in glasses remain a matter of open discussion, while a good knowledge of the complex environments of metal ions is important for understanding the composition dependence of glass properties like optical basicity, ion transport and viscosity. Valuable information about the nature of metal ion sites in glass can be extracted from infrared spectra because the vibrations of metal ions around their stable local sites give strong absorption bands in the far-infrared region [8]. In most ionic oxide glasses, the analysis of the asymmetric far-infrared profiles supports the existence of at least two distinct distributions of metal ions sites [9, 10]. This 'two-site' model for modifying cations was interpreted on the basis of the chemical versatility of the glass networks to provide sites for metal ions with variable coordination number and anionic charge density [9, 10].

In the present work we review far-infrared spectroscopy results on alkali borate glasses and discuss the implications of the types of cation site on optical basicity and ion transport properties of glasses. To shed light on the microstructure of the metal ion sites, we discuss also molecular dynamics data on Li-borate glasses with particular emphasis on the types of site occupied by Li cations and their dynamic response.

2. METAL ION-SITE VIBRATIONS BY FAR-INFRARED SPECTROSCOPY

Borate glasses can be considered as prototypes for applying far-infrared spectroscopy to study metal ion-site interactions in glass. This is because boron has the smallest mass compared to other network forming elements, and therefore the main vibrational modes associated with the glass network appear above ca. 500 cm^{-1} and are well separated from the metal ion-site vibrational modes active in the far-infrared region. Figure 2 shows far-infrared absorption spectra of glasses having the triborate composition, M_2O-$3B_2O_3$, where M is an alkali metal. All infrared data were collected using the specular reflectance technique, which has the potential to yield high quality spectral data from the same sample form and in a continuous frequency range (ca. 25 - 4000 cm^{-1}). The real and imaginary parts of the complex refractive index of glasses were obtained by the Kramers-Kronig transformation of the reflectance data, and were employed to calculate the absorption coefficient spectra shown in Figure 2 (for experimental and computational details see publications in refs. [9,10]).

The far-infrared spectra of Figure 2 show the typical asymmetric profiles observed in earlier studies of alkali borate glasses by either reflectance [10] or transmission [9,11] spectroscopy. To investigate the source of far-infrared absorption in ionic glasses the spectral profiles have been deconvoluted into Gaussian type bands, using standard non-linear least squares fitting with a minimum number of bands [9,10]. The frequencies of the resulted component bands, marked by H and L in Figure 2, are plotted in Figure 3 versus the square root of the inverse metal ion mass, $M_C^{-1/2}$. Frequency data for alkaline earth ions in metaborate glasses, MO-B_2O_3 with M = Mg, Ca, Sr and Ba, are plotted in the same figure for comparison with the alkali borate system [12]. A good linear dependence of ν_H and ν_L on $M_C^{-1/2}$ has resulted for both glass systems suggesting that bands L and H should be related to oscillatory modes which involve mainly the motion of metal ion.

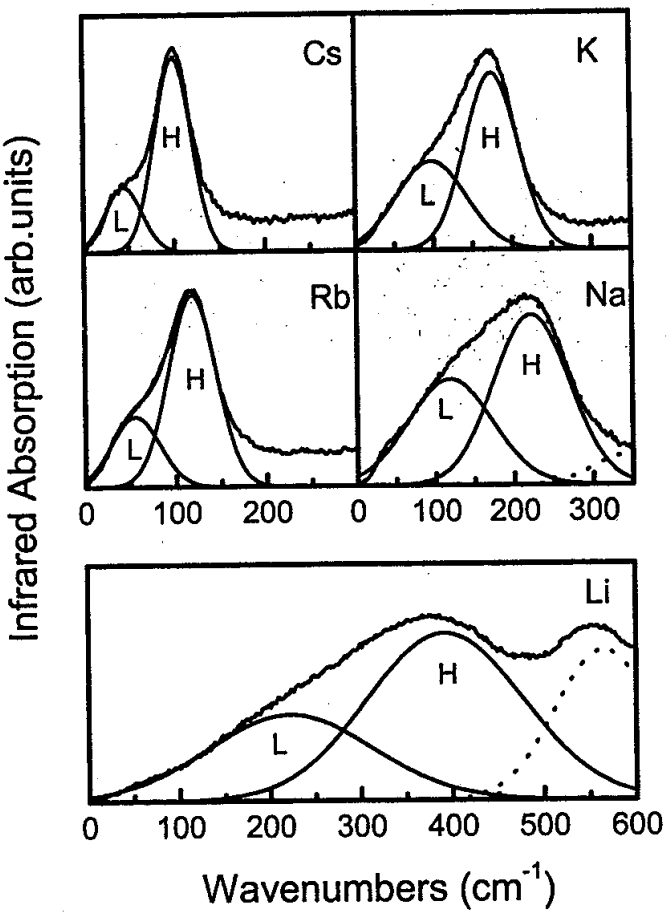

Figure 2. Far-infrared absorption spectra of M_2O-$3B_2O_3$ glasses, M = Li, Na, K, Rb and Cs, deconvoluted into Gaussian component bands.

The oscillatory motion of a metal ion relative to its site should be compensated by an appropriate motion of oxygen atoms forming the site, so that there is no net displacement of the center of mass of the metal ion/site complex. Although the reduced mass of metal ion-site vibration, μ, depends on the mass of metal ion and oxygen atom in a way determined by the symmetry of the site [9,10], Figure 3 shows that the metal ion has a predominant contribution on the oscillation frequency. Therefore, we may approximate the reduced mass with the metal ion mass, $\mu \approx M_C$, which implies that the cation vibrates against an infinitely heavy and quite rigid anionic site. This approximation is appropriate because the anionic sites consist of oxygen atoms which are connected to larger network segments through B-O bonding.

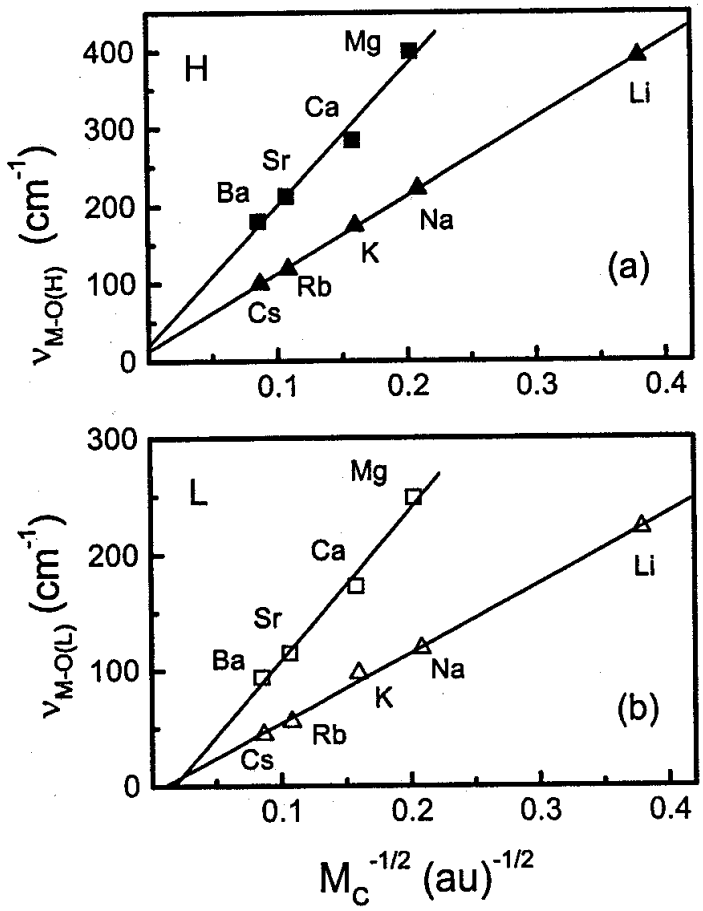

Figure 3. Metal ion-site vibration frequencies versus the square root of the inverse metal ion mass, $M_C^{-1/2}$, for alkali triborate (M = Li, Na, K, Rb and Cs) and alkaline earth metaborate (M = Mg, Ca, Sr and Ba) glasses [13]. Frequencies denoted by $\nu_{M-O(H)}$ (a) and $\nu_{M-O(L)}$ (b) correspond to band maxima of components H and L, respectively, which were obtained from fitting the far-infrared spectra (e.g. in Figure 2). Lines are least square fittings.

As shown in Figure 3, the frequencies of vibration of alkaline earth ions against their sites are higher compared to those of alkali ions of similar mass, suggesting different force constants of the metal-oxygen bonding in the two families of glasses. In order to explore the factors determining the force constant of metal ion-site vibration in glass, a Born-Mayer-type potential was be employed to model the cation-site interactions [9,13]. It was shown that the force constant of cation-site vibration for a metal cation of charge q_C occupying a site of anionic charge q_A is given by the expression:

$$f = \frac{\alpha\, q_C\, q_A}{3\, r_0^3} \left(\frac{r_0}{\rho} - 2\right) \qquad (1)$$

where r_0 is the equilibrium metal ion-oxygen distance, ρ is the repulsion parameter between charges at short distances, and α is the pseudo-Madelung constant in the Born-Mayer-type potential. Thus, the charges of site and cation and the equilibrium cation-oxygen distance are the key bonding parameters determining the force constant of cation-oxygen (site) vibration.

On the basis of eq. 1 and the fact that the frequency of metal ion-site vibration, ν_{M-O}, is proportional to $(f/\mu)^{1/2}$, we may now explain the observed differences between the vibration frequencies of alkaline earth, $\nu_{M^{2+}-O}$, and alkali metal cations, $\nu_{M^{+}-O}$, in their equilibrium sites. Assuming alkaline earth and alkali metal ions of the same mass and of nominal charges +2 and +1, respectively, and corresponding metal ion-site force constants $f_{M^{2+}-O}$ and $f_{M^{+}-O}$, we may write:

$$\frac{\nu_{M^{2+}-O}}{\nu_{M^{+}-O}} = \left(\frac{f_{M^{2+}-O}}{f_{M^{+}-O}}\right)^{1/2} \approx \left(\frac{q_{M^{2+}}\, q_{site\, M^{2+}}}{q_{M^{+}}\, q_{site\, M^{+}}}\right)^{1/2} \approx 2 \qquad (2)$$

It was assumed above that there is charge neutrality at the metal ion-site level, i.e., the absolute value of the product of charges of metal ion and its site can be approximated by the square of metal ion charge. The square roots of force constants can be obtained directly from the linear fits of the frequency data in Figure 3, and this leads to $(f_{M^{2+}-O}/f_{M^{+}-O})^{1/2}$ being equal to 1.8 for the H-type bands and 2.1 for the L-type bands. This is a very satisfactory result considering all the approximations made.

To highlight the strong influence of cation mass and charge on the metal ion-site vibration frequency, we show in Figure 4 the same frequency data versus the product $q_M\, M_C^{-1/2}$. It is very interesting to find that the H- and L-band frequency data collapse on two different lines, with the one for ν_H showing the larger slope. Although variation of the metal oxide content would lead to changes in the metal ion-site vibration frequencies [9,10], the ν_H and ν_L frequency data would still be grouped around two lines with different slopes in their dependence on $q_M\, M_C^{-1/2}$. Therefore, in accordance with earlier reports [9,10] we may suggest that H and L bands should originate from metal ion vibrations in two distributions of anionic sites in glass. The question then concerns the difference of these two type of anionic environments that leads to the appearance of two far-infrared component bands.

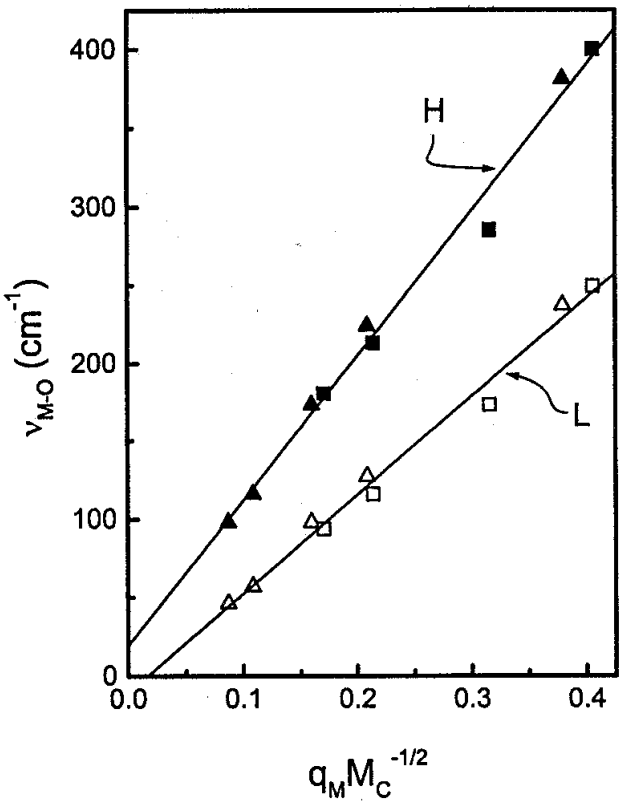

Figure 4. Metal cation-site vibration frequencies, $\nu_{M\text{-}O}$, versus $q_M M_C^{-1/2}$, where q_M and M_C are the charge and mass of metal ion in alkali, $M_2O\text{-}3B_2O_3$, and alkaline earth, $MO\text{-}B_2O_3$, borate glasses [13]. Nominal charges of metal ions and atomic ion masses were used. Filled and empty symbols represent $\nu_{M\text{-}O(H)}$ and $\nu_{M\text{-}O(L)}$ frequencies, with squares and triangles corresponding to alkaline earth and alkali metal ions, respectively. Lines are least square fits to frequency data.

To address this problem we have considered recently the possibility of multiple occupancy around certain anionic sites [13]. Elliott and co-workers [14] argued that the strength of the Coulomb repulsive forces between metal cations coordinated to the same anionic site will most likely restrict the site occupancy to two cations around a site. Treating the case of two metal cations vibrating at opposite positions of an anionic environment, we could demonstrate that the far-infrared results in Figure 4 are compatible with attributing bands L and H to singly- and doubly-occupied metal ion sites, respectively [13]. It is obvious that sites with different cation occupancy will exhibit different anionic charge density, and this would be reflected on glass properties sensitive to anionic charge distribution. In the following section we discuss the consequences of metal ion site distinction on the glass optical basicity.

3. LOCAL OPTICAL BASICITY IN BORATE GLASSES

Anionic sites with different electron density are expected to exhibit different electron donating ability, and, therefore, different basicity. Duffy and Ingram have expressed the electron donating ability of a medium in terms of its optical basicity, Λ [15]. This quantity is obtained experimentally from the frequency of the $^1S_0 \rightarrow {}^3P_1$ ultraviolet absorption band of probe ions with s^2 electronic configuration, i.e., Tl^+, Pb^{2+}, Bi^{3+}, doped in the medium. In recent investigations of alkali and alkaline earth borate glasses [16] we have established a simple relationship between the metal ion-site vibration frequency and the optical basicity of glass:

$$\nu_{eff} = \alpha + \beta \Lambda \qquad (3)$$

where ν_{eff} represents the effective frequency of the metal ion-site vibration when the cation occupies an "average" type of site in the glass. This effective frequency is obtained in terms of ν_H and ν_L by:

$$\nu_{eff} = (f_H \nu_H^2 + f_L \nu_L^2)^{1/2} \qquad (4)$$

where the weighting factors f_H and f_L are approximated by $f_{H(L)} = A_{H(L)} / (A_H + A_L)$; with A_H and A_L being the integrated intensities of the H and L ion-site vibration bands, respectively.

For glasses in the xNa_2O-$(1-x)B_2O_3$ system, the analysis of the far-infrared data have shown that $\alpha = -74$ cm^{-1} and $\beta = 468$ cm^{-1} [16]. As indicated above, the types of anionic sites hosting Na^+ ions (sites H and L) should have different basicity. The local basicity of each site can be calculated from eq. (3) by substituting ν_H and ν_L for ν_{eff}. The resulting values are denoted by $\Lambda_{H,calc}$ and $\Lambda_{L,calc}$ and are shown in Figure 5 as a function of the Na_2O content [16]. It is obvious that the two types of site have distinctly different local optical basicity, especially at high sodium oxide contents. Figure 5 shows also the local basicities ($\Lambda_{H,,Tl}$ and $\Lambda_{L,Tl}$) obtained from the two components of the UV absorption band of Tl^+ probe ions introduced in sodium borate glasses from their melt state [15]. It is remarkable that the local basicities signalled by the UV probe ion (Tl^+) are in very good agreement with those obtained from the vibration frequencies of the far-infrared probe ion (Na^+). It is of interest to note that Hosono et al. [17] have also interpreted their ESR spectra on a variety of Tl-doped ionic oxide glasses (including borates, germanates and silicates) in terms of two distinct sites for the thallous ions.

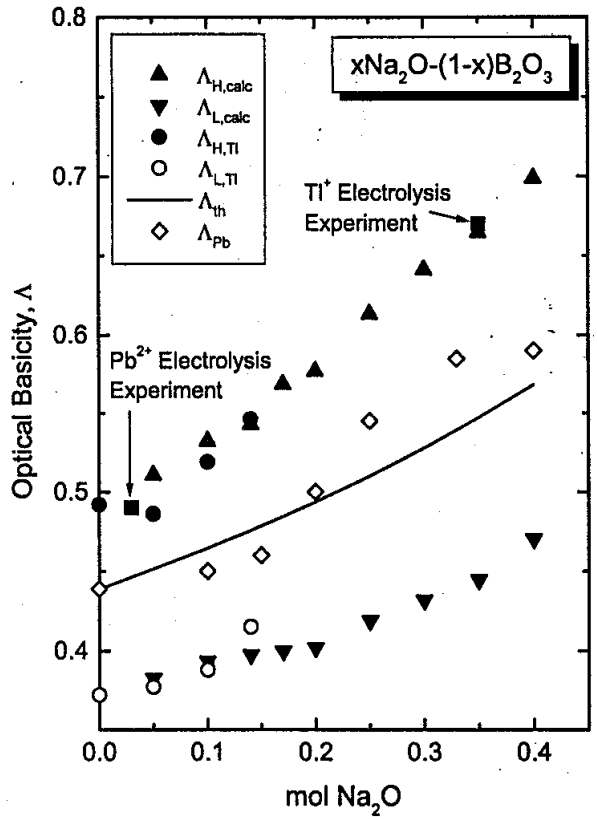

Figure 5. Calculated optical basicities of the two types of site, $\Lambda_{H,calc}$ and $\Lambda_{L,calc}$, versus the Na_2O content in Na-borate glasses [16]. Optical basicities obtained from the UV of Tl^+ ($\Lambda_{H,Tl}$ and $\Lambda_{L,Tl}$) and Pb^{2+} (Λ_{Pb}) probe ions introduced in the glass from the molten state are also shown. The points marked by 'Tl^+ electrolysis experiment' and 'Pb^{2+} electrolysis experiment' are calculated from the UV spectra of Tl^+ and Pb^{2+} ions electrolysed in the corresponding Na-borate glass [18]. The theoretical optical basicity, Λ_{th}, is calculated from the expression $\Lambda_{th} = 1.15\,[x/(3-2x)] + 0.439\,[3(1-x)/(3-2x)]$, where 1.15 and 0.439 are the basicities of Na_2O and B_2O_3, respectively [16].

Relevant to ion transport properties are the two experimental points in Figure 5 labelled by 'Tl^+/Pb^{2+} electrolysis experiment'. These points mark the experimental UV optical basicities registered by Tl^+/Pb^{2+} probes introduced into sodium borate glasses by electrolysis experiments reported by Baucke and Duffy [18]. The basicities indicated by both probes are very close to the high optical basicity obtained from the ν_H frequency of Na^+ ions ($\Lambda_{H,calc}$), and considerably higher than the 'average' or theoretical optical basicity of the glass, Λ_{th}. These findings may be interpreted as indicating that the more mobile sodium ions, which are presumably replaced by Tl^+/Pb^{2+} ions during electrolysis, are mainly the Na^+ ions occupying sites of high basicity (H-type sites). This point will be addressed further in terms of the molecular dynamics results presented in the next section.

Finally, we note that Figure 5 shows that dipositive probe ions (Pb^{2+}) introduced in Na-borate glasses from the molten state signal basicities different from those of the unipositive ions (Tl^+/Na^+ probes). The implications of such results are discussed in details elsewhere [16].

4. METAL ION SITES BY MOLECULAR DYNAMICS SIMULATIONS

As presented above, far-infrared and UV probe ion spectroscopy show the presence of two types of metal ion sites in borate glasses. In this section we discuss the microstructure of these anionic sites hosting the metal ions on the basis of recent results of a molecular dynamics (MD) study of lithium borate glasses. This MD investigation of xLi_2O-$(1-x)B_2O_3$ glasses covers broad composition ($0.2 \leq x \leq 0.5$) and temperature (300 to 1250 K) ranges [19], but the present work focuses on characteristic results for the $x = 0.3$ composition. Details on the potential employed and the computational and data analysis procedures are reported elsewhere [19].

The MD study showed that the short-range order (SRO) structure of the $x = 0.3$ glass consists of neutral borate triangles with all oxygen atoms being bridging, $B\emptyset_3$ ($\emptyset$ = bridging oxygen, BO), charged borate triangles with two bridging and one non-bridging oxygen, $B\emptyset_2O^-$ (O = non-bridging oxygen, NBO), and charged borate tetrahedra with four BO's, $B\emptyset_4^-$. These SRO structures of the glassy network provide the sites which accommodate the metal ions. In equilibrium, the Li^+ ions tend to reside in local minima of the potential energy surface associated mainly with the negatively charged SRO structural units, such as $B\emptyset_4^-$ and $B\emptyset_2O^-$. Representative snapshots of the $x = 0.3$ glass structure generated from the atomic coordinates at 300 K are shown in Figure 6 and demonstrate typical anionic sites for the lithium ions.

Close examination of the simulated structure in Figure 6a shows that the Li ion site is formed by eight nearest neighbour oxygen atoms within a radius of 3 Å; four of them are bridging oxygens belonging to two $B\emptyset_4^-$ units and the other four are bridging oxygens from $B\emptyset_3$ units. Such sites where only bridging oxygen atoms constitute the coordination sphere of the Li ion are designated as bridging-type (b-type) sites, and the Li ion occupying the site is labelled Li^b. The typical characteristic of b-type sites is that each $B\emptyset_4^-$ unit has on the average one Li^b neighbour and each Li^b is coordinated to oxygen atoms of two $B\emptyset_4^-$ units. Therefore, a b-type site can be regarded as a singly occupied site.

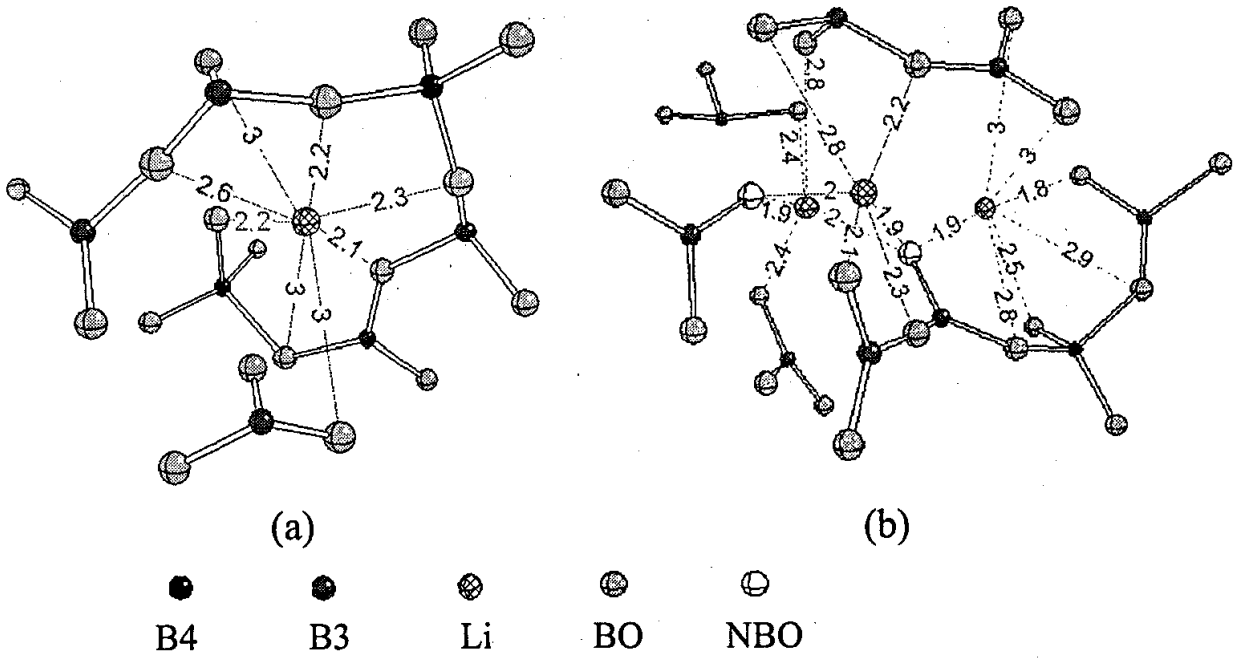

Figure 6. Details of the simulated atomic-scale structure at 300 K of the $0.3Li_2O$-$0.7B_2O_3$ glass revealing the presence of (a) bridging-type, and (b) non-bridging-type coordination environments for Li ions [13,19]. Distances between Li ions and oxygen atoms in the first coordination shell within a radius of 3 Å are included. Boron-oxygen bonds are shown by double solid lines, B4 and B3 denote 4- and 3-fold coordinated boron atoms and BO and NBO are for bridging and non-bridging oxygen atoms, respectively.

The segment of the structure shown in Figure 6b provides sites for three Li ions. The two Li ions at the left are in sites which involve two NBO's each and three or four BO's within a radius of 3Å. Thus, six- and five-fold coordination environments for Li ions are formed with average Li-O bonding distances of 2.2 and 2.3 Å, for these particular sites. The site of Li ion in the right of Figure 6b involves one NBO and six bridging oxygen atoms, three of which are bonded to a $B\emptyset_4^-$ unit. Therefore, all three Li ion sites in Figure 6b involve NBO atoms of $B\emptyset_2O^-$ units in addition to the bridging oxygen atoms. Such sites are denoted as non-bridging type (nb-type) sites and the corresponding lithium ions are labelled Li^{nb}. The characteristic of nb-type sites in Figure 6b is that each NBO is coordinated to two Li ions at a distance 1.9 to 2.0 Å. In that respect, nb-type sites can be considered as doubly occupied sites.

The structural differences between b-type and nb-type sites are reflected on the Li-O partial radial distribution functions (RDF). As shown elsewhere [13,19], the partial Li^{nb}-O RDF peaks at 1.92 Å and is better defined than the partial Li^{b}-O RDF at 2.12 Å. This is reasonable since the Li^{nb}-O RDF accounts for both Li^{nb}-BO and Li^{nb}-NBO bonding, whereas Li^{b}-O RDF involves only Li^{b}-BO bonding. Also, the coordination number, CN, of oxygen around Li^{nb} is found to be about

5.5 when a cut-off distance of 3.0 Å is used, while CN ≈ 8 is obtained for oxygen around Li^b and a cut-off distance of 3.3 Å. These results show clearly that sites hosting Li^{nb} ions are better defined compared to anionic sites of Li^b ions.

The differences in bonding characteristics of Li^{nb} and Li^b ions are manifested in their short-time dynamics determining the lithium-oxygen vibrational properties. We can now examine the vibrational properties of Li ions in their b- and nb-type sites through the velocity autocorrelation function, $\Phi(t)$:

$$\Phi(t) = \left\langle (1/N) \sum_{j=1}^{N} \vec{v}_j(t) \cdot \vec{v}_j(0) \right\rangle \qquad (5)$$

where $\vec{v}_j(t)$ is the velocity of metal ion j at time t and N is the number of metal ions [20]. The vibrational density of states, $\Phi(\omega)$, which reflects the vibrational properties of metal ions can be obtained directly from the Fourier transform of $\Phi(t)$. This approach has been applied separately to Li^{nb} and Li^b ions [19] and the calculated $\Phi(\omega)$ spectra are shown in Figure 7a for x = 0.3 and T = 300 K. The calculated $\Phi(\omega)$ spectra associated with Li^{nb}-site and Li^b-site vibrations are in the far-infrared region, with both spectra being quite broad but well separated from each other. A key finding is the fact that the spectrum of Li^{nb} ions appears at higher frequencies compared to that of Li^b ions. This is the case also with other lithium borate glass compositions investigated by molecular dynamics [19]. These results are in full agreement with the nature of sites hosting lithium ions and the discussion in section 2 concerning the vibration frequencies of cations in singly- and doubly-occupied anionic sites. Indeed, comparison with the deconvoluted experimental spectrum in Figure 7b shows that bands L and H can be associated mainly with the $\Phi(\omega)$ spectrum of Li^b and Li^{nb} ions, respectively. Thus, the MD results provide insights for the microscopic origin of component band L and H in the experimental far-infrared spectra.

In addition to differences in their far-infrared response, Li^{nb} and Li^b ions were shown to exhibit distinct behaviour in their long-time dynamics, as well. In particular, it was found that the mobility of Li ions in nb-type site environments is considerably larger than that of Li ions residing in b-type sites. This result is in good agreement with the response of Tl and Pb probe ions electrolysed in borate glasses, which appear to have moved along sites of high optical basicity, i.e., H-type or nb-type sites (see previous section). A complete account of the Li ion dynamics on the basis of the MD investigation will be presented elsewhere [21].

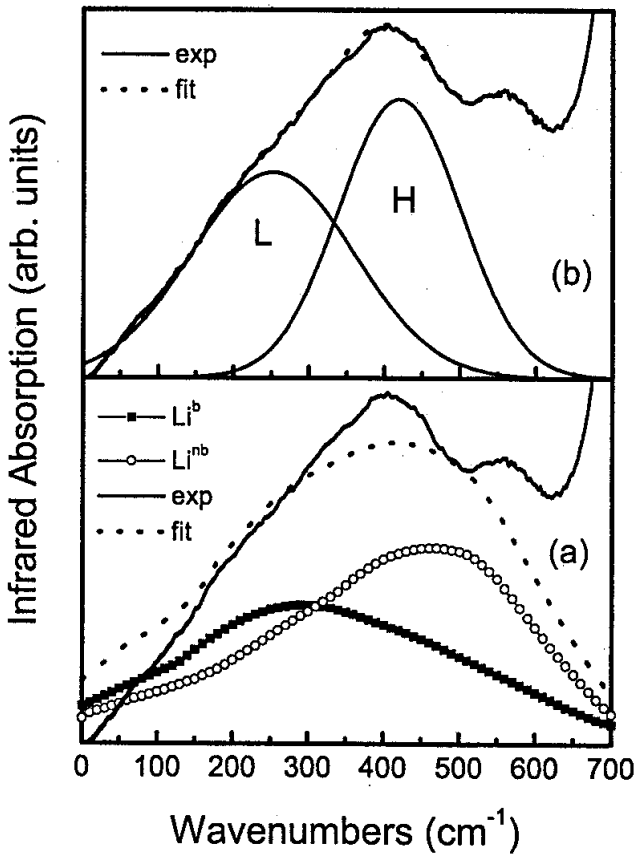

Figure 7. (a) Calculated power spectra $\Phi(\omega)$ of lithium ions residing in bridging-type (Li^b) and non-bridging-type (Li^{nb}) environments in the $0.3Li_2O$-$0.7B_2O_3$ glass at 300 K. A linear combination of the two power spectra is shown for comparison with the experimental far-infrared spectrum of the same glass. The experimental spectrum (b) has been deconvoluted into Gaussian components L and H, which show close correspondence with the power spectra of cations Li^b and Li^{nb}, respectively [13,19].

Useful information about the distribution of cation sites and the cation-site interaction energy in ionic solids and be obtained also by dielectric spectroscopy, including the Complex Impedance Spectroscopy (CIS) and the Thermally Stimulated Current (TSC) techniques. These approaches were employed recently to study metal ion sites in silicate [22] and borate glasses [23] as an alternative tool to far-infrared spectroscopy. Analysis of the dielectric data in the form of energy distribution functions showed the presence of two major dipolar reorientation responses, manifesting the distribution of metal ions over at least two types of metal ion sites. This is in agreement with the results of far-infrared and probe ion spectroscopy and molecular dynamics studies discussed in this work.

5. CONCLUDING REMARKS

This paper reviews recent findings concerning the nature of sites hosting metal ions in ionic glasses. Particular emphasis is placed on borate glasses because they are the most suitable systems for far-infrared studies. It was shown that the far-infrared response convolutes at least two contributions originating from metal ion-site vibrations. The origin of these lower- (L) and higher- (H) frequency contributions was discussed on the basis of a Born-Mayer-type potential for the metal ion-site interactions, and it was suggested that the L and H bands can be associated with oscillations of metal ions against their singly- and doubly-occupied sites, respectively.

The conclusions drawn from far-infrared spectroscopy are in line with findings of other experimental techniques such as dielectric and UV probe ion spectroscopy. In particular, the local optical basicities (Λ_H, Λ_L) calculated from the Na^+ ion-site (oxygen) vibration frequencies were found to be very similar to those obtained by UV spectroscopy of Tl^+ ions doped in the borate glass from the melt. However, when the Tl^+ and Pb^{2+} probes are introduced in the glass by electrolysis they signal basicities characteristic of high basicity (Λ_H) sites, suggesting that such site environments facilitate ionic motion.

The structure of the short-range order borate units forming the anionic sites of lithium ions was revealed by molecular dynamics simulations on Li-borate glasses. It was found that bridging oxygen atoms from $B\emptyset_4^-$ and $B\emptyset_3$ units constitute the singly-occupied or bridging-type sites, whereas non-bridging oxygen atoms of $B\emptyset_2O^-$ units together with bridging oxygens are involved in the establishment of doubly-occupied or non-bridging-type sites. The calculated power spectra of Li ions in bridging- and non-bridging-type sites were found to correspond very well to the experimental L- and H-component bands of the Li-site vibrational activity in the far-infrared. The 'two-site' model for binary borate glasses discussed in this work incorporates elements of the earlier continuous random network and modified random network models.

ACKNOWLEDGEMENTS

I am grateful to Drs. C.P. Varsamis, A. Vegiri, A.P. Patsis, Y.D. Yiannopoulos and G.D. Chryssikos for their involvement in various parts of the work reviewed here, and to Professors J.A. Duffy and M.D. Ingram for many fruitful discussions over the years on several points presented in this paper.

REFERENCES

[1] W.H. Zachariasen, J. Am. Chem. Soc. 54 (1932), 3841.

[2] B.E Warren, J. Biscoe, J. Am. Ceram. Soc. 21 (1938), 259; B.E. Warren, J. Am. Ceram. Soc. 24 (1941), 256.

[3] G.N. Greaves, J. Non-Cryst. Solids 71 (1985), 203; G.N.Greaves, K.L. Ngai, Phys. Rev. B. 52 (1995), 6358.

[4] M.C. Eckersly, P.H. Gaskell, A.C. Barnes, P. Chieux, Nature 335 (1988), 525; P.H. Gaskell, M.C. Eckersly, A.C. Barnes, P. Chieux, Nature 350 (1991), 675.

[5] C. Huang, A.N. Cormack, J. Chem. Phys. 93 (1990), 8180; H. Melman, S. Garofalini, J. Non-Cryst. Solids 134 (1991), 107; B. Vessal, G.N. Greaves, P.T. Marten, A.V. Chadwick, R. Mole, S. Houde-Walter, Nature 356 (1992), 504; J. Oviedo, J.F. Sanz, Phys. Rev. B. 58 (1998), 9047.

[6] N.M. Vedishcheva, B.A. Shakhmartin, M.M. Shultz, B. Vessal, A.C. Wright, B. Bechra, A.G. Clare, A.C. Hannon, R. Sinclair, J. Non-Cryst. Solids 192&193 (1995), 292.

[7] B. Gee, H. Eckert, J. Phys. Chem. 100 (1996), 3705.

[8] G.J. Exarhos, W.M. Risen, Solid State Commun. 11 (1972), 755; G.H. Exarhos, P.J. Miller, W.M. Risen, J. Chem. Phys. 60 (1974), 4145; B.N. Nelson, G.J. Exarhos, J. Chem. Phys. 71 (1979), 2739; E.I. Kamitsos, M.W. Risen, J. Non-Cryst. Solids 65 (1984), 333; C.I. Merzbacher, W.B. White, J. Non-Cryst. Solids 130 (1991), 18.

[9] E.I. Kamitsos, J. Phys. Chem. 93 (1989), 1604; E.I. Kamitsos, J. Physique IV C2 (1992), 87.

[10] E.I. Kamitsos, A.P. Patsis, M.A. Karakassides, G.D. Chryssikos, J. Non-Cryst. Solids 126 (1990), 52; E.I. Kamitsos, A.P. Patsis, G.D. Chryssikos, J. Non-Cryst. Solids 152 (1993), 246; E.I. Kamitsos, Y.D. Yiannopoulos, H. Jain, W.C. Huang, Phys. Rev. B 54 (1996), 9775; E.I. Kamitsos, G.D. Chryssikos, Solid State Ionics 105 (1988), 75; G.D. Chryssikos, L. Liu, C.P. Varsamis, E.I. Kamitsos, J. Non-Cryst. Solids 235 (1998), 761; C.P. Varsamis, E.I. Kamitsos, G.D. Chryssikos, Phys. Rev. B. 60 (1999), 3885.

[11] C. Liu, C.A. Angell, J. Chem. Phys. 93 (1990), 7378.

[12] Y.D. Yiannopoulos, G.D. Chryssikos, E.I. Kamitsos, Phys. Chem. Glasses 42 (2001), 164.

[13] E.I. Kamitsos, C.P. Varsamis, A. Vegiri, Proc. Int. Congr. Glass Vol. 1 (2001), p.p. 234-246.

[14] R.J. Elliott, L. Perondi, R.A. Barrio, J. Non-Cryst. Solids 168 (1994), 167.

[15] J.A. Duffy, M.D. Ingram, J. Am. Chem. Soc. 93 (1971), 6448; J.A. Duffy, M.D. Ingram, J. Non-Cryst. Solids 21 (1976), 373; M.D. Ingram, J. Non-Cryst. Solids 222 (1997), 42.

[16] J.A. Duffy, G.D. Chryssikos, E.I. Kamitsos, Phys. Chem. Glasses 36 (1995), 53; E.I. Kamitsos, G.D. Chryssikos, A.P. Patsis, J.A. Duffy, J. Non-Cryst. Solids 196 (1996), 249; J.A. Duffy, B. Harris, E.I. Kamitsos, G.D. Chryssikos, Y.D. Yiannopoulos, J. Phys. Chem. 101 (1997), 4188.

[17] H. Hosono, H. Kawazoe, J. Nishii, T. Kanazawa, J. Non-Cryst. Solids 51 (1982), 217.
[18] F.G.K. Baucke, J.A. Duffy, J. Electrochem. Soc.127 (1980), 2230; F.G.K. Baucke, J.A. Duffy, J. Chem. Soc. Faraday Trans. I 79 (1983), 661.
[19] C.P. Varsamis, A. Vegiri, E.I. Kamitsos, Cond. Matter Phys. 4 (2001), 119.
[20] A.H. Verhoef, H.W. Hartog, J. Non-Cryst. Solids 182 (1995), 235; A. Karthikeyan, P. Vinatire, A. Levasseur, K.J. Rao, J. Phys. Chem. B. 103 (1999), 6185.
[21] C.P. Varsamis, A. Vegiri, E.I. Kamitsos, Phys. Rev. B 65 (2002) 104203.
[22] F. Henn, S. Devatour, L. Maati, J.C. Giuntini, H. Schaefer, J.V. Zanchetta, J. Vanderschueren, Solid State Ionics 136-137 (2000), 1335.
[23] S. Devautour, C.P. Varsamis, F. Henn, E.I. Kamitsos, J.C. Giuntini, J.V. Zanchetta, J. Vanderschueren, J. Phys. Chem. B. 105 (2001), 5657.